energies

MDPI

Article

Experimental Investigations and Modeling of Atmospheric Water Generation Using a Desiccant Material

Ahmed Almasarani [1], Imtiaz K. Ahmad [2], Mohamed F. El-Amin [3,4,*] and Tayeb Brahimi [3]

[1] Energy Engineering, College of Engineering, Effat University, Jeddah 21478, Saudi Arabia
[2] Natural Sciences, Mathematics and Technology Unit, College of Engineering, Effat University, Jeddah 21478, Saudi Arabia
[3] Energy Research Lab, College of Engineering, Effat University, Jeddah 21478, Saudi Arabia
[4] Mathematics Department, Faculty of Science, Aswan University, Aswan 81528, Egypt
* Correspondence: momousa@effatuniversity.edu.sa; Tel.: +966-54-256-7083

Abstract: Harvesting atmospheric water by solar regenerated desiccants is a promising water source that is energy-efficient, environmentally clean, and viable. However, the generated amounts of water are still insignificant. Therefore, more intensive fundamental research must be undertaken involving experiments and modeling. This paper describes several experiments, which were conducted to predict and improve the behavior of water absorption/desorption by the Calcium Chloride ($CaCl_2$) desiccant, where the uncertainty did not exceed $\pm 3.5\%$. The absorption effect in a deep container was studied experimentally and then amplified by pumping air into the solution. The latter measured water absorption/desorption by a thin solution layer under variable ambient conditions. Pumping air inside deep liquid desiccant containers increased the water absorption rate to 3.75% per hour, yet when using a thin layer of the solution, it was found to have increased to 6.5% per hour under the same conditions. The maximum amount of absorbed water and water vapor partial pressure relation was investigated, and the mean absolute error between the proposed formula and measured water content was 6.9%. An empirical formula, a one-dimensional mathematical model, was then developed by coupling three differential equations and compared to experimental data. The mean absolute error of the model was found to be 3.13% and 7.32% for absorption and desorption, respectively. Governing mathematical conservation equations were subsequently formulated. The mathematical and empirical models were combined and solved numerically. Findings obtained from the simulation were compared to experimental data. Additionally, several scenarios were modeled and tested for Jeddah, Saudi Arabia, under various conditions.

Keywords: atmospheric water harvesting; desiccant; water content; relative humidity

Citation: Almasarani, A.; Ahmad, I.K.; El-Amin, M.F.; Brahimi, T. Experimental Investigations and Modeling of Atmospheric Water Generation Using a Desiccant Material. *Energies* **2022**, *15*, 6834. https://doi.org/10.3390/en15186834

Academic Editor: Carlo Roselli

Received: 18 August 2022
Accepted: 14 September 2022
Published: 19 September 2022

1. Introduction

Water is the world's most precious resource yet is becoming increasingly scarce due to the competing demands of the world's burgeoning population. Finding solutions to the water crisis that the world is currently facing is a significant challenge, as is the need for greatly improved global equitable and sustainable water resources management. To date, water desalination is the most viable solution, but it has a large ecological footprint, as it is energy-intensive and environmentally taxing. Heightened water requirements for domestic water supply, sanitation, and irrigation purposes, are the leading causes of stress on the global availability of water [1]. Such water-fueled stress has serious social, economic, and developmental implications. The United Nations (UN) reported that 2.2 billion people lack access to safely managed drinking water, more than 3.6 billion people do not have adequate sanitation, and more than 2.3 billion people do not have basic hygiene facilities [2]. Adopted by the UN Member States in 2015 at the UN Summit, the Sustainable Development Goals (SDGs) of the 2030 Agenda for Sustainable Development seek to reduce global poverty and achieve enhanced worldwide prosperity. SDG 6 relates specifically to

providing the sustainable management of clean water and sanitation for all. Such is the importance of water; it is the common theme in almost all the SDGs. It is essential to food security (SDG 2); health and sanitation (SDGs 3 and 6); energy, employment, and industries (SDGs 7, 8, and 9); climate, and the protection of ecosystems (SDGs 13, 14, and 15) [3]. The Middle East and North Africa (MENA) region is the planet's most arid terrain mainly due to harsh weather conditions, increasing dependence on imported water bottles, and seawater desalination [4]. Annual freshwater withdrawals refer to total water withdrawals from renewable aquifers used in all sectors such as agriculture, industry, and municipal or domestic. It is noteworthy that most MENA countries fall in the extremely high-stress region where the withdrawal is more than 100% of the renewable sources, and seawater desalination is involved in covering the shortage [5], see Figure 1. With an ever-increasing population and rising water demands, it is predicted to confront severe water shortages and even warmer climates [3]. Of particular concern in this region are the water-intensive methods used in agriculture and the energy-intensive method in desalination [6].

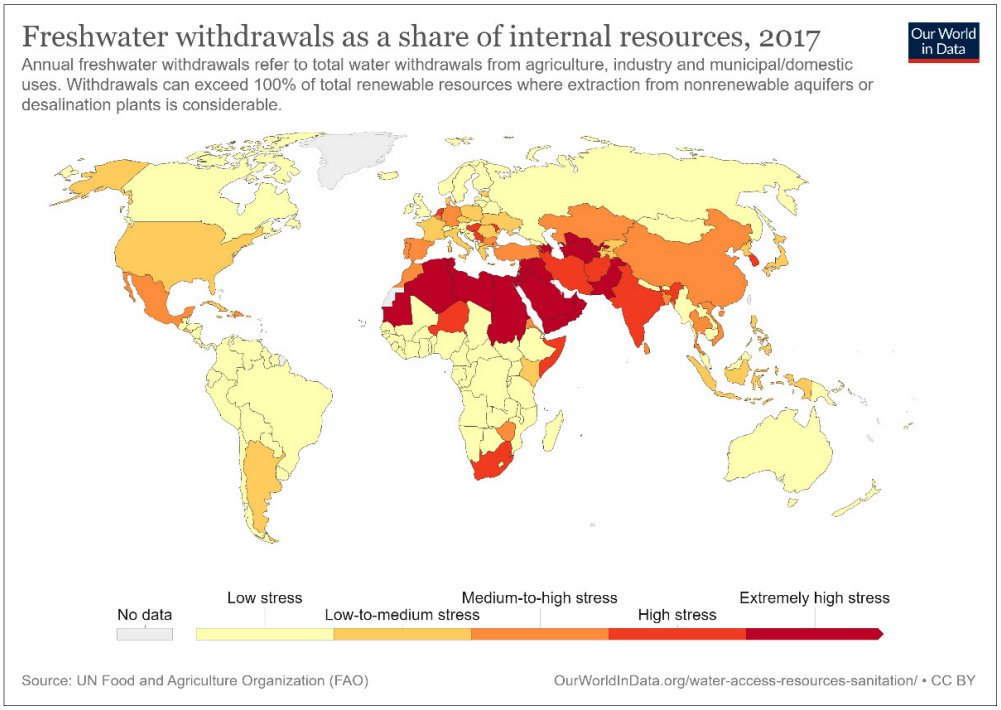

Figure 1. Freshwater withdrawals as a share of internal resources, 2017 [5].

The world will continue to face significant challenges where the water supply is limited, and the quality is variable unless a sustainable water source can be found and managed efficiently. The sole source of accessible water on the planet is moisture in the air [7], and it is thought that approximately 13 sextillions (13×10^{21}) L of water exist in the atmosphere at any given time [8]. To date, harvesting water from the atmosphere occurs using three processes and is a promising solution to the world's water crisis [9]. One such method involves desiccant materials that act as absorbents of atmospheric moisture and from which water vapor is then released. This research presents the results of experiments conducted to assess and optimize the behavior of Calcium Chloride desiccant as a means of efficient Atmospheric Water Harvesting (AWH).

The following section, Section 2, contains a literature review on atmospheric water generation using hygroscopic salts; Section 3 outlines the materials and methodology used in the different experiments; Section 4 presents the results and discussion and highlights the main findings of this study. In Section 5, we present an empirical mathematical formula. Conservation governing equations have been developed and solved numerically in

Section 6. Several scenarios were simulated and discussed in Section 7. Finally, conclusions are drawn in Section 8.

2. Literature Review

In recent years, AWH has gained popularity due to the rising water shortage problem, stressed water systems, issues in public water infrastructure, and natural disasters [4]. As mentioned previously, in recognizing the increasing challenge of water shortage, in 2015, the UN established SDG 6 (among 17 SDGs) to "Ensure availability and sustainable management of water and sanitation for all" [2]. In 2018, the UN launched the Water Action Decade 2018–2028 to make significant progress toward sustainable development [10]. Because the quantity of fresh water available on Earth is just 2.5% compared to 96.54% of salty water in oceans, seas, and bays [7], significant efforts have been devoted to harvesting water from clouds, fog, or atmospheric water vapor, particularly in dry regions [8–12]. Two main methods of atmospheric water generators have been used for atmospheric harvesting water: passive and active methods [13,14]. With passive techniques, water may accumulate naturally without needing an external power source, relying only on natural temperature variations. The most employed passive method is a fog catcher, which generates a reasonable amount of water [8,15,16]. However, they only work in a limited number of geographical areas and are restricted to specific climate conditions such as high humidity. Besides, fog collection technology only contributes a little to alleviating water shortages.

In contrast, active methods used for AWH are not restricted to a specific location and are less affected by site or climate conditions. Still, they require an external source of energy, such as solar energy. Atmospheric water generators can use solar energy (refrigeration-based) or solar thermal (sorption-based) energy. The amount of water generated depends on relative humidity and ambient temperature.

Bar [17] patented a three-stage process technology that extracts water from the air. A solid desiccant absorbs humidity, and a heat pump heats it to desorb water vapor. Then the vapor turns to water by passive condensation. Such a system is environmentally friendly due to moderate low-cost heating (solar or waste heat). With a low energy consumption of 100–150 kcal/L, the system generates water at a rate of 1000 L/day. Extracting water by cooling air to the dew point produces low water output in passive techniques and consumes high energy with active techniques. Alternative methods that capture water molecules regardless of the dew point are more energy-efficient, especially at low relative humidity [11]. Membrane-assisted humidity harvesting is an active method that depends on mechanical energy (vacuum pump) to push water molecules through a selective membrane and then condense it to produce water. With the help of a low-pressure sweep stream, the membrane-assisted device harvests an average amount of 3.36 L/day [18].

Because of the abundance of solar energy, solar-driven hygroscopic water harvesting is increasingly scrutinized, as researchers are working on improving structural designs, sorbents' capacity, and thermal management [13,14,19]. Many challenges are still observed with these types of Atmospheric Water Generators (AWG), such as increasing efficiency, scalability, and cost reduction. This implies ensuring that research should focus on the microscopic mechanism of the process, develop new hygroscopic agents, modify solar absorbers, and design new condensation systems. Talaat et al. [20] tested a double-cycle absorbent-based water harvester where the cycles alternate between day and night. At night, the apparatus exposes the Calcium Chloride ($CaCl_2$) solution to natural humid air. In the daytime, the system is covered with a double-faced transparent surface, forcing the water vapor to desorb due to high temperature, which then condenses on the cover sides and is collected inside a bottle. This system is affected by weather and ambient conditions, generating a maximum amount of water of 0.63 L/day. Sleiti et al. [21] recommended multiple layers of stacked high-quality sorbent to improve the water output of the AWG unit. A layer of 25 mm thickness of silica gel generated around 0.8 L/day, and the unit consisted of a water sorbent bed, condenser, radiant heat flux, and reflector. Due to different experimental conditions such as ambient temperature, relative humidity, silica gel thickness,

surface area to volume ratio, and radiant heat flux, the amount of water recovered varies. Increasing the radiant flux will reach peak efficiency and then drop; the relative humidity is proportional to water capture.

Solar-driven hygroscopic AWGs' water production depends on external environmental and internal device factors. Understanding the interaction between external and internal factors such as temperature, pressure, wind speed, relative humidity, sorbent characteristics, types of solar collectors, and condenser design is the key to manufacturing an effective scaled-up product in the future. These parameters may only affect the production rate or maximum sorbent capacity or affect both rate and capacity. In the case of desiccants' absorption, maximum water absorption is related to their inherent characteristics and the surrounding environment. Changing the chemical properties of the desiccant or making a physical modification to the system, such as using a porous medium as a host, will increase the water uptake.

Several studies demonstrate that some changes may increase the water uptake but decrease the absorption rate, as in the work of Zhang et al. [22]. They used porous silica gel as a host for $CaCl_2$, but the equilibrium process took 35 h, while using carbon nanotubes only took 4 h. Moreover, a composite of 85% $CaCl_2$ and 15% Lithium Bromide (LiBr) was found to absorb three times its weight, while $CaCl_2$ alone only absorbed twice its own weight [23]. Experiments of Elashmawy et al. [24] clearly demonstrated the effect of increasing the temperature of the saturated sorbent by adding a solar parabolic concentrator to the tubular solar-still with a $CaCl_2$ trough inside and increasing its temperature to 98 °C, thereby tripling water production to 2.4 $L/m^2/day$. One of the advantages of using desiccants instead of cooling to dew point is that the cooling method loses its reliability below 30% relative humidity. On the other hand, most desiccant-based AWGs succeeded in generating a reasonable amount of water in low relative humidity conditions.

Sorbent characteristics can differ between absorption and desorption; one such example is the absorption rate of Lithium Chloride (LiCl), which is higher than $CaCl_2$ but lower in the desorption phase [25]. In some ways, the carrying capacity factors (temperature, relative humidity) may also affect the process rate. However, on the other hand, factors such as surface area, wind velocity, and liquid desiccant flow are only related to how fast/slow the sorbent will reach equilibrium. Liquid desiccants have excellent flexibility with respect to their surface area, and can adopt many host surfaces, such as porous silica gel and carbon nanotubes, as mentioned earlier [22]. Elashmawy et al. [26] used a black cotton cloth as a host for their experiments and collected 1.06 $L/m^2/day$ using five shelves, to increase surface area. This can be compared to a 1 kg flat layer of saw wood with a 10–40 μm distance hosting a 60% concentration of $CaCl_2$, which only collected around 0.18 $L/m^2/day$ [27]. Furthermore, the sand hosting 37% $CaCl_2$ concentration solution was able to generate 0.11 $L/m^2/day$ with the help of a solar Scheffler reflector [28]. Since the sorbent creates a low vapor pressure area around its surface, water molecules in the air will move to fill it; therefore, circulating more water molecules over the surface of the sorbent will speed up the saturation. In the city of Hail (northern Saudi Arabia), a forced airflow was injected in solar-still tubes containing black cotton cloth impregnated with $CaCl_2$ solution via small fans at different speeds. The highest absorption amount was from the sample subjected to the fastest fan (4 m/s) and collected 0.47 $L/m^2/day$ [24]. It was thought that the absorption rate of $CaCl_2$ solution fluctuated due to the wind speed in Dhahran, the eastern region of Saudi Arabia. This was verified by an experiment that demonstrated that the high flow of the desiccant solution achieved the highest absorption rate of 2.11 L/m^2 at night. The opposite happened with regard to desorption during the daytime, where the lower flow rate caused a greater amount of collected water [29].

Before utilizing desiccants to generate freshwater from the air, researchers focused on the desiccants' industrial and air conditioning properties [16,30,31]. Properties such as solubility, solution vapor pressure, density, surface tension, viscosity, and thermal conductivity are essential to understanding the behavior of the desiccant solution at various concentrations and in certain environments. Thus, despite recent studies on AWG, utilizing

desiccants in the AWG field requires conducting further detailed experimental investigations. Moreover, from the aspect of mathematical modeling, few studies have been conducted to study atmospheric water harvesting in recent years. Milani et al. [32] developed a model for a complete dehumidification system using TRNSYS software. Sibie et al.'s [33] modeling and simulation focused on Copper Chloride ($CuCl_2$), Copper Sulfate ($CuSO_4$), and Magnesium Sulfate ($MgSO_4$) anhydrous salts and introduced an analytical solution for the mathematical model. Furthermore, Alkinani et al. [34] developed a $CuCl_2$ water vapor absorption mathematical model. The experiments in this paper aim to discover $CaCl_2$ desiccant behavior under AWH-related conditions and provide a mathematical model describing the AWH behavior, thereby enhancing the absorption and desorption processes that can be applied to various liquid desiccants.

3. Materials and Experimental Methods

Deliquescent substances such as $CaCl_2$ dissolve in the absorbed water and keep absorbing in the liquid form until saturation. The concentration is calculated using molarity (mol/L) or by $CaCl_2$ mass fraction of the total solution (m_s/m_{sol}) and presented as a water-to-salt mass ratio. It is defined as the mass of water divided by the mass of desiccant material (see Equation (1)). When preparing the $CaCl_2$-water solution, using dihydrate Calcium Chloride ($CaCl_2 \cdot 2H_2O$), a correction is made by adding the mass of two water molecules to the solvent volume in the concentration calculation.

$$\theta = \frac{m_{water}}{m_{desiccant}} \cdot 100\% \quad (1)$$

3.1. Instruments and Uncertainty Analysis

The experimental set-up was designed to measure basic absorption/desorption phenomena using calibrated instruments with small acceptable errors. A temperature and humidity logger (Tzone, Multi-use USB Temp&RH Data Logger, Shenzhen, China) was used to measure both temperature and relative humidity. It measures the temperature with an accuracy of ± 0.5 °C and relative humidity with an accuracy of $\pm 3\%$. The resolution for the readings is 0.1 for both temperature and relative humidity. The analytical balance used is from the GR Series-Model GR-200, by A&D Company, Tokyo, Japan. It automatically self-calibrates using an internal/external weight and can correct the internal weight to within ± 1.5 mg.

An experiment was conducted specifically to determine the uncertainty. Seven identical dishes were filled with the same amount and concentration of distilled water and Calcium Chloride. These samples were exposed to the same ambient conditions as for the previous experiments, and the water-to-mass ratio was measured every hour. Since the starting point was set to the same conditions, the uncertainty was 0%, and after a few hours, the measurements started to deviate from the mean value (see Figure 2a). Finally, the maximum standard deviation for the water-to-salt mass ratio did not exceed $\pm 3.5\%$ of the mean value of all the measurements (see Figure 2b). Thus, this percentage will reduce the accuracy of the model compared to the ensuing experimental measurements.

3.2. Absorption Rate Experiments

3.2.1. Passive Absorption

The most recent studies demonstrate that a thin desiccant layer is usually used to maximize the surface area in order to increase the absorption rate [8,12]. The effect of the surface area-to-depth ratio needs to be investigated further to understand the reported decrease in absorption rate and water uptake of desiccants while increasing the thickness. Therefore, two beakers of the same size (100 mL) with different amounts of $CaCl_2$ solution were left in an outdoor shaded area in Jeddah, KSA. The average ambient temperature and humidity were 28 °C and 61%, respectively. The mass of the samples, temperature, and relative humidity were measured every hour. The two beakers, designated A and B, each had a surface area of 0.002 m^2 and 10 g of $CaCl_2$ with 5 mL of distilled water and 20 g of

$CaCl_2$ with 10 mL of distilled water, respectively. The water–mass ratio of the solution in both beakers was 50% (see Figure 3).

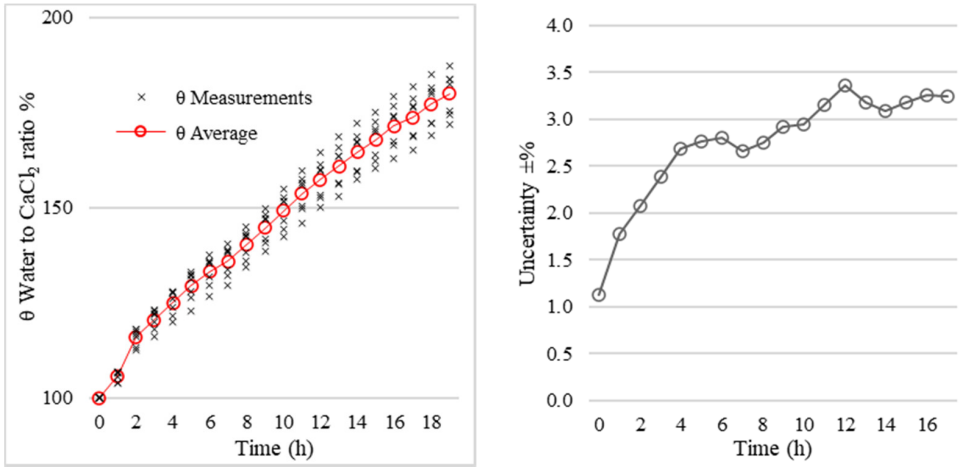

Figure 2. (**a**) Average of water-to-salt mass ratio measurements. (**b**) Uncertainty of water-to-salt mass ratio measurements.

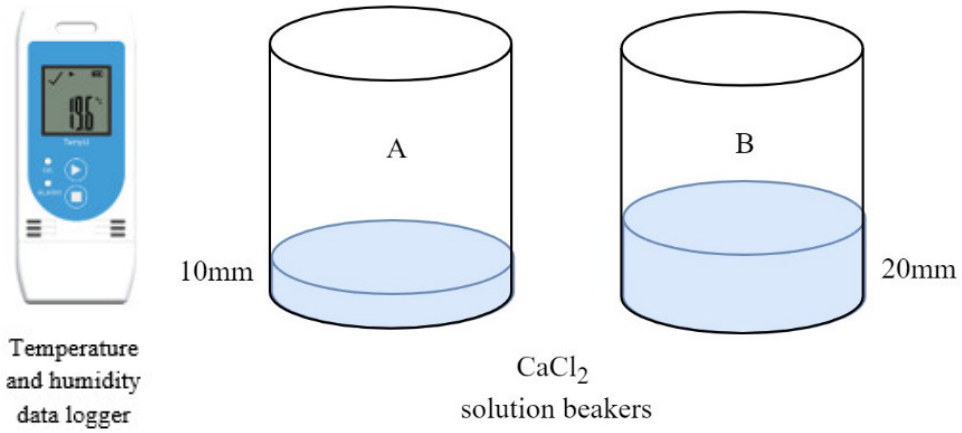

Figure 3. Experimental setup to investigate the effect of solution depth on absorption, (**A**) 10 mm, and (**B**) 20 mm $CaCl_2$ solution depth.

3.2.2. Active Absorption

Previous studies [22,31] reported how the absorption rate decreases exponentially with time; the way to overcome this is to use fans or pumps [26,29]. The decrease in absorption rate is much higher when the depth of the solution is increased, so it was decided to improve the absorption by injecting air through the solution. The purpose of the pumped air was to increase the airflow and surface area, and equilibrate the solution. For this, two 60 mL syringes (A and B) were employed (see Figure 4). Syringe A was tightly sealed at the bottom using a silicon gun and plastic cover. In contrast, syringe B was first connected to one 2.5 W/250 L/H air pump, then afterward, it was simultaneously connected to two pumps. A one-way valve was added to syringe B to prevent the $CaCl_2$ solution from leaking into the air tube, and a rubber cap was used to close the syringe at the top to prevent any loss of solution. The airflow was allowed to exit from a small hole in the side of syringe B. A solution of $CaCl_2$ was prepared and distributed evenly between containers A and B. The temperature and relative humidity were measured at intervals by a TZ-TempU03 Temperature and Humidity data logger [35].

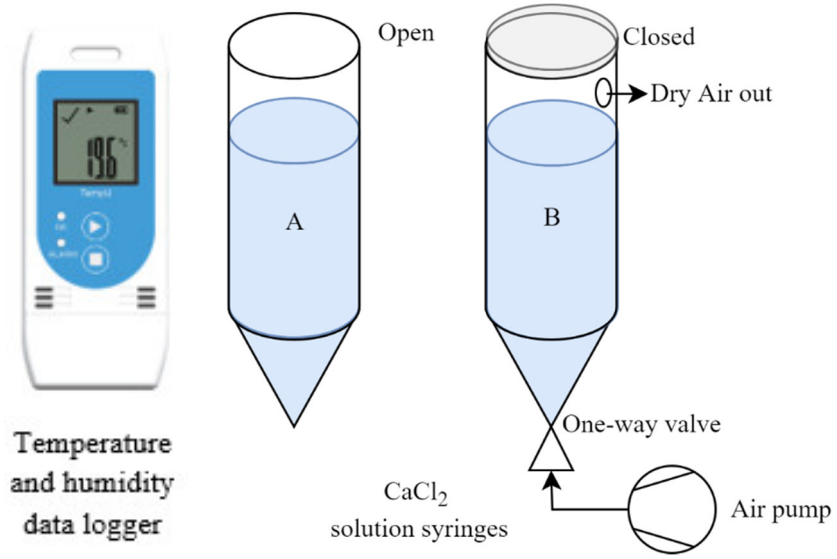

Figure 4. Experimental set-up to increase absorption rate in $CaCl_2$ solution with (**A**) natural, and (**B**) forced air flow.

3.3. Saturation-Point Experiments

3.3.1. Saturation under Similar Ambient Conditions

The ability of a desiccant to absorb moisture depends on the partial pressure of water vapor in the air, as the presence of a desiccant creates low water vapor pressure that attracts water molecules in the air. At a certain point known as saturation, the solution reaches a dynamic equilibrium (steady-state) with the surrounding air, and a continuous exchange of water molecules occurs. Thus, any change in the air temperature or relative humidity will affect the water vapor partial pressure and the concentration of the desiccant solution. To verify this, a thin layer of $CaCl_2$ solution with a fan was used to measure saturation points, which were compared with the $CaCl_2$ vapor–liquid equilibrium phase diagram in Ref. [30].

3.3.2. Saturation under Different Ambient Conditions

As mentioned above, any air temperature or relative humidity change will be reflected in the $CaCl_2$ solution concentration. However, in the case of heating or cooling the solution without changing the ambient temperature, the concentration will adjust to balance the change in the solution vapor pressure. The dynamic equilibrium point for a heated solution of $CaCl_2$ was investigated, without impacting ambient temperature, in order to measure its effect on the $CaCl_2$ concentration. For this experiment, a hotplate was used to heat a saturated $CaCl_2$ solution, and a fan was used to circulate the ambient air above the solution. Desorption of the water content was measured every hour until equilibrium occurred. The ambient temperature and humidity were recorded along with the related moisture content.

4. Results and Discussion

While preparing the $CaCl_2$ solution, which is a very exothermic reaction, it was observed that the heat generated from the reaction affected the first few hours of the sorption process. This can be interpreted as the solution started to desorb water instead of absorbing it, as shown at the start of the graph in Figure 5. It is useful to consult the solid–liquid equilibrium (SLE) boundary diagram of $CaCl_2$ [30] before preparing the desiccant solution to avoid a highly diluted or crystallized solution.

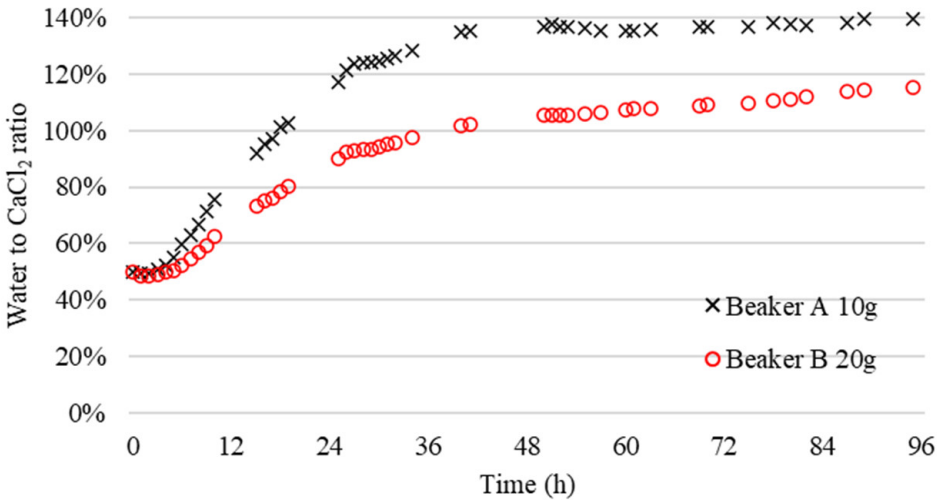

Figure 5. The effect of desiccant depth on $CaCl_2$ absorption.

4.1. Absorption and Desorption Rate

In the initial experiment, the absorption behavior of the $CaCl_2$ solutions was investigated and the results are presented in Figure 5. Data from this experiment show the effect of solution depth on desiccant absorption while maintaining the same surface area. The depth of the solution in beakers A and B was 0.01 and 0.02 m, respectively. The $CaCl_2$ in beaker A reached a water content of 140% of the $CaCl_2$ mass. Moreover, the amount of absorbed water in sample A was more responsive to ambient temperature fluctuations. Therefore, liquid desiccants, such as $CaCl_2$, placed in deep containers, favor using active circulating pumps.

Similarly, the absorption rate significantly decreased inside the syringe with the larger desiccant depth. Table 1 shows the initial and final water levels compared to the ratio of the solution over a period of 4 h. The average absorption rate with a 100 mm diameter thin layer was 6.50% per hour, while the syringe connected to two air pumps was only 3.75%. Air pumped throughout the solution generated a lot of small, isolated drops that adhered to the syringe's walls, while others evaporated from the hole in the side.

Table 1. Absorption rate with different configurations.

Sample	Initial Water (%)	Final Water (%)	Change (%)	Average Change (%)/h
No pump	57	58	1	0.25
1 pump	57	68	11	2.75
2 pumps	42	57	15	3.75
Thin layer	42	68	26	6.50

The pumped air created an airflow, which when coupled with a large surface area, increased the absorption rate of the desiccant compared to the passive syringe. However, it was found to be slower than that of the passive thin layer. Moreover, the presence of pumped air converted the relation between time and moisture absorption to a linear relation, resulting in a larger absorption difference at each desiccant concentration. The passive thin layer reached saturation long before the active syringe, even when it was equipped with two air pumps (see Figure 6).

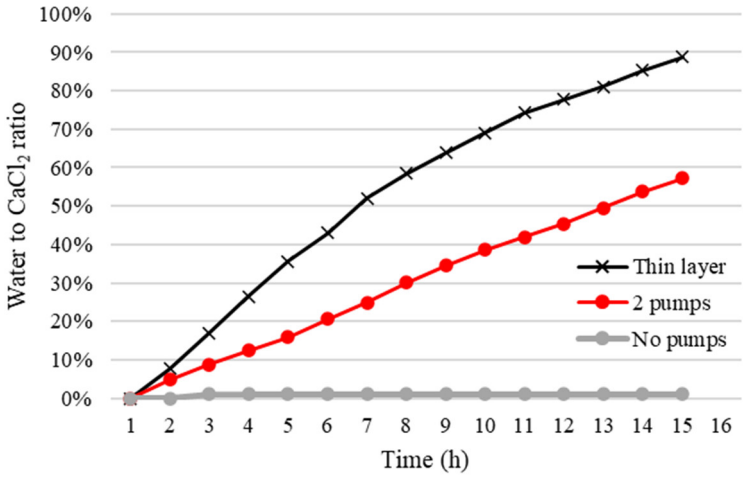

Figure 6. The effect of a thin layer and air pumps on $CaCl_2$ absorption rate.

4.2. Vapor–Liquid Dynamic Equilibrium

Vapor–liquid equilibrium begins at the saturation point of the desiccant. Each ambient condition allows the $CaCl_2$ to absorb a certain amount of water vapor. Phase diagrams of the $CaCl_2$ solution vapor pressure demonstrate the relation of $CaCl_2$ mass fraction-to-water vapor partial pressure as a function of temperature and relative humidity [30,31]. Since the reported values in these diagrams represent saturation points inside closed climate chambers, such values will not be valid for an open variant system such as an atmospheric water harvester. Thus, to produce more reliable data for this research, we measured many equilibrium points under different ambient conditions. After comparing 40 measurement points with the known phase diagram, we found that the measurements in this study follow a similar pattern as the known phase diagram and indicate an average difference of 65% less water ratio than the amount reported in the phase diagram (see Figure 7). As expected, this discrepancy is due to the closed environment of the climate chambers, where the temperature, humidity, and pressure are maintained automatically, and there is no wind movement.

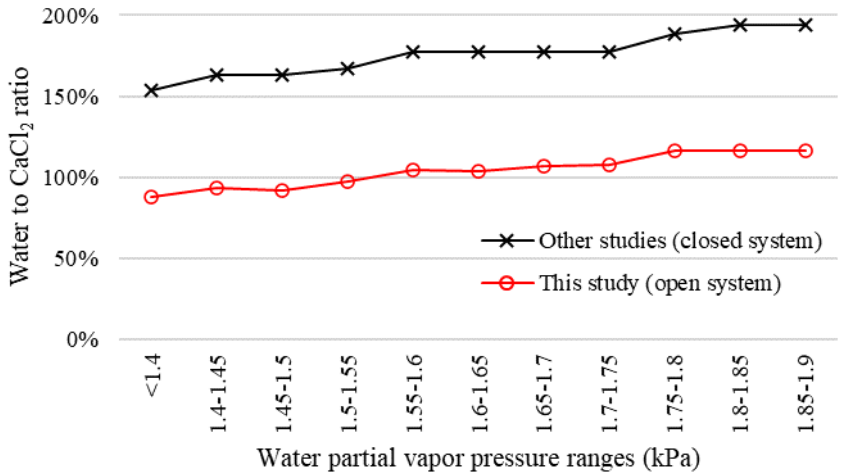

Figure 7. A comparison of water content measurements with the phase diagram in other studies [30,31].

Moreover, we investigated the saturation point at various solution temperatures under different ambient conditions. A hotplate, operated at 35 °C, was employed to desorb the water from a saturated $CaCl_2$ solution. Upon completion, the mass was recorded at every change in temperature and relative humidity over 24 h. Further trials were conducted at 40 °C, 45 °C, and 50 °C (see Figure 8). Increasing the solution temperature in the open system significantly reduced the saturation point compared to the saturation in the closed

systems reported in [30,31]. Thus, the high desorption amounts of water in the open system are promising for increased water collection.

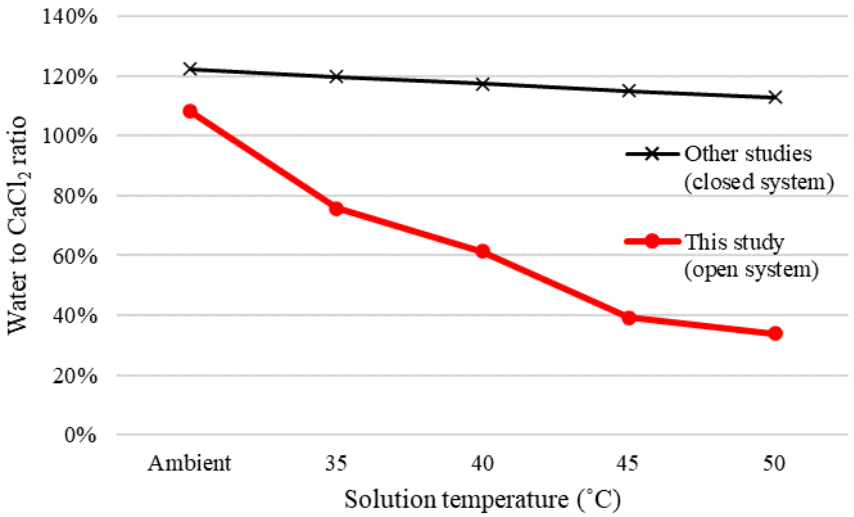

Figure 8. Comparison of the average water content when the solution temperature is the same as ambient temperature (25 ± 2 °C) [30,31], and when they are different (this study).

To explore further the behavior of $CaCl_2$, the measured temperatures of 35 °C, 45 °C, and ambient temperature were used to investigate the effect of relative humidity on the saturation point. Increasing the solution temperature by 10 °C reduced the water content by an average of 32% even at high ambient relative humidity values (see Figure 9).

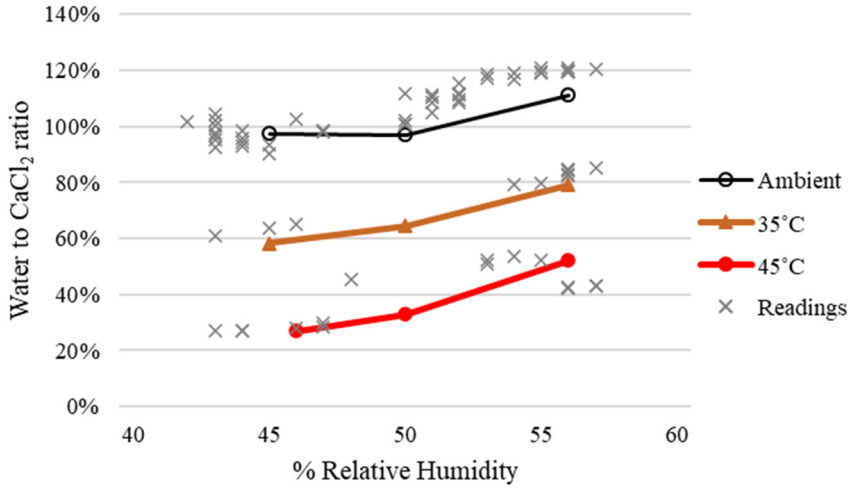

Figure 9. Average $CaCl_2$ water content against % relative humidity at different solution temperatures (ambient temperature = 25 ± 2 °C).

5. Proposed Formulas

The exponential decay equation is commonly used in modeling chemical reactions, electrostatics, heat transfer, and optics. By reviewing the experimental data, the desiccant appears to follow an exponential decay function in both forms, decay for desorption and growth for absorption. $CaCl_2$ and similar desiccants may also follow the curve of the exponential decay/growth function shown in Figure 10. Internal factors can be thought of as the type of desiccant, solubility, surface area, and depth. External factors are assumed to be temperature, relative humidity, and wind velocity (airflow).

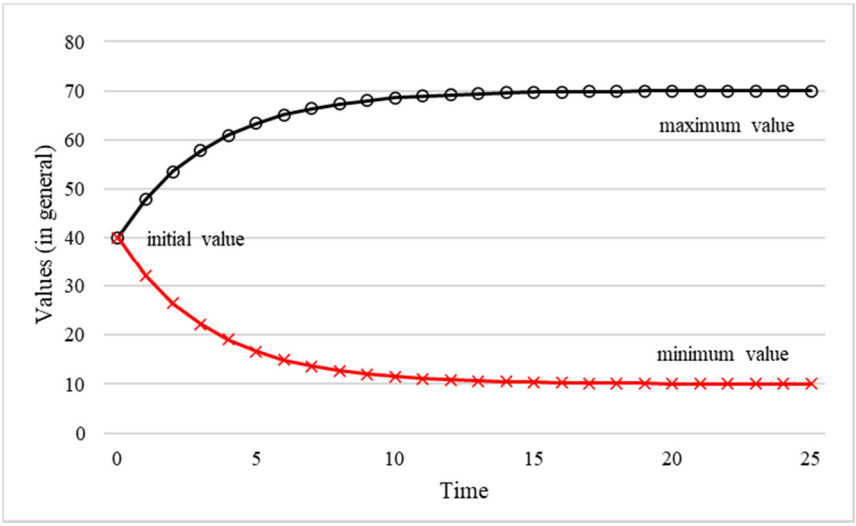

Figure 10. General exponential decay/growth curves.

On considering relevant internal and external factors affecting both absorption and desorption, the formula that describes this study's experimental data on $CaCl_2$ can be expressed as the following:

$$\theta = \theta_{max} + (\theta_0 - \theta_{max})e^{-bt} \tag{2}$$

where

$$\theta_{max} = (c_1 P_w + c_2)(1 + \frac{\ln \tau}{\ln \tau + c_3}) \tag{3}$$

$$\tau = \frac{T_{amb}}{T_{sol}} \tag{4}$$

$$P_w = RH\ P_s\ 100\% \tag{5}$$

$$P_s = \frac{\exp\left(34.494 - \frac{4924.99}{T+237.1}\right)}{(T+105)^{1.57}} \qquad (T > 0\ ^\circ\mathrm{C}) \tag{6}$$

where θ equals the mass ratio of water-to-$CaCl_2$ after elapsed time t and θ_0 is its initial value, b is a variable related to the absorption/desorption rate due to temperature. The ratio of ambient temperature and solution temperature is τ. T is the temperature in Celsius and RH is the relative humidity. The computation of the saturation water vapor pressure, P_s, at a given temperature, has been adopted from the work of Huang [36]. His formula is less complicated than previous ones, with a lower error. P_w is the water vapor partial pressure in kPa.

Finally, θ_{max} is the maximum amount of water ratio the salt can absorb in a certain ambient condition, in other words, the vapor–liquid dynamic equilibrium points at a particular condition. The θ_{max} equation is derived based on the observation of the linear relationship between θ_{max} and water vapor pressure.

The equation's constants $c_1 - c_3$ are optimized using the Generalized Reduced Gradient (GRG) algorithm [37]. The convergence is set to 0.0001, the start set to multi, and the derivative is set to central. The target was to minimize the average absolute error between measured saturation points and the θ_{max} equation output.

The mean absolute error (MAE) was found to be 6.9%. As the temperature of the solution increases, the values deviate from the actual readings due to crystallization (see Figure 11). The constants $c_1 - c_3$ generated and found by the optimization are presented in Table 2.

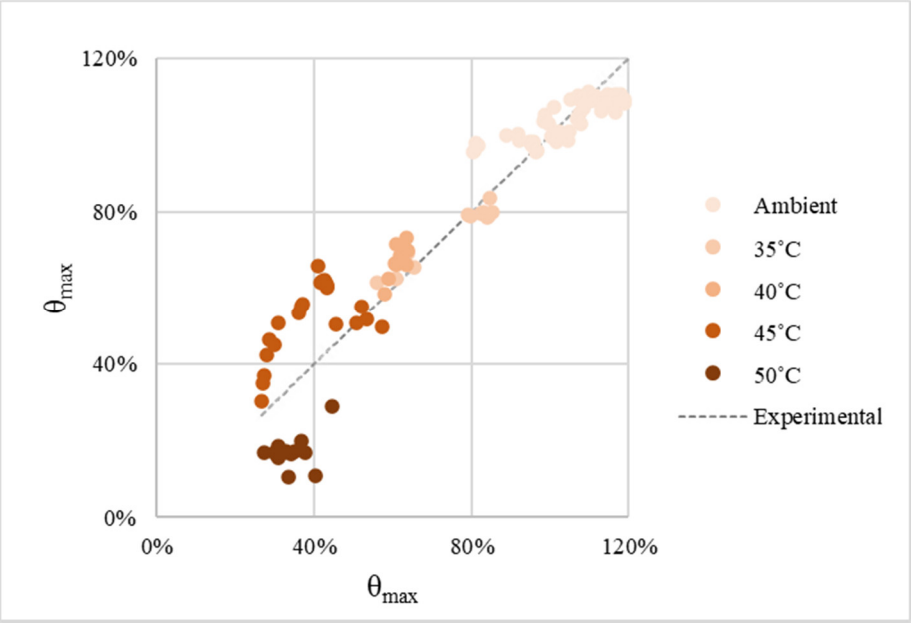

Figure 11. $CaCl_2$ maximum water uptake (θ_{max}) at different temperatures (ambient temperature = 25 ± 2 °C).

Table 2. Constants related to the $CaCl_2$ maximum water–mass ratio uptake.

Constant	c_1	c_2	c_3
Value	0.4297	0.3221	1.5163

It appears that the proposed formula describes the absorption process better than the desorption process. The formula predicted the water absorbed during the day (see Figure 12) more accurately than the desorbed amount when the solution is heated up to 45 °C (see Figure 13). This implies that for calculating θ_{max}, the initial water content is required.

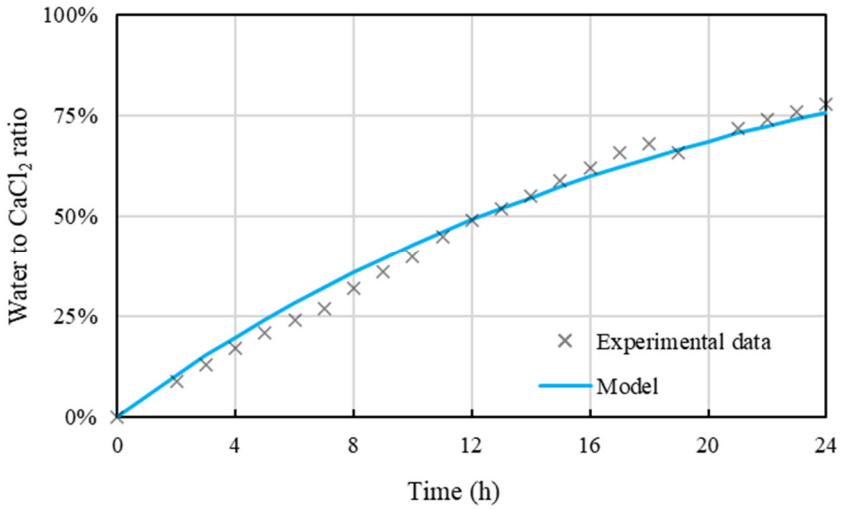

Figure 12. Logistic growth/decay model for $CaCl_2$ moisture absorption.

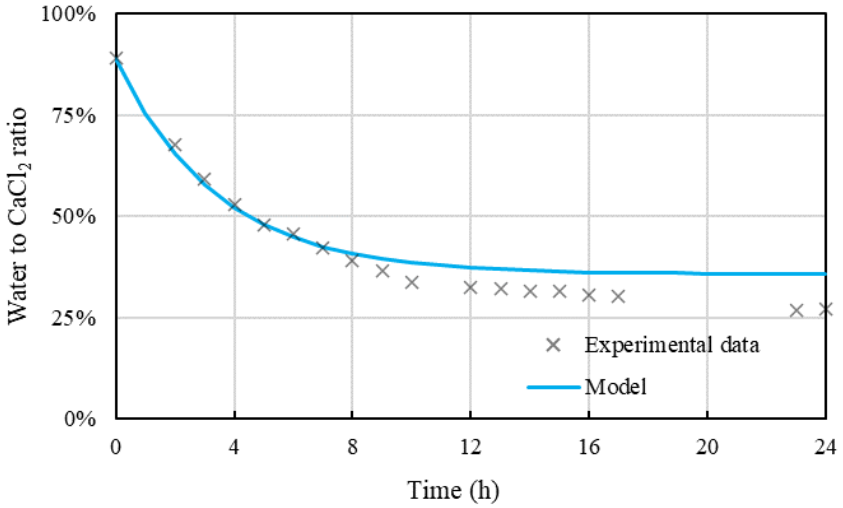

Figure 13. Exponential decay/growth model for $CaCl_2$ moisture desorption.

The mean absolute error for the formula in the absorption process was 1.9% after fixing b to equal 0.05 (see Figure 14a). The same formula gave a MAE of 3.56% in the desorption process after b was set at 0.294 (see Figure 14b).

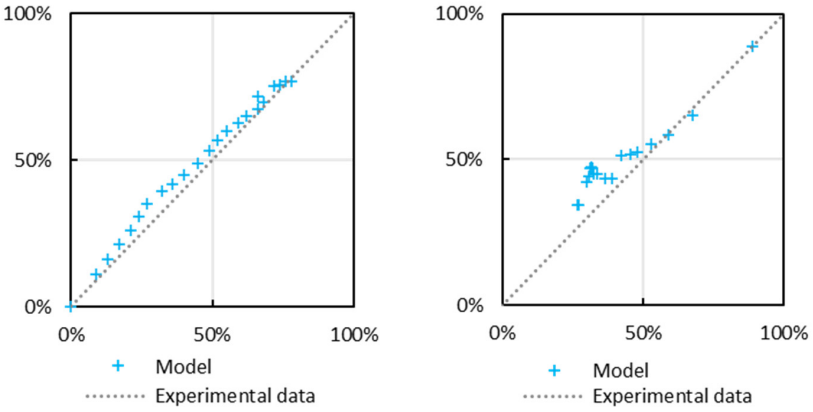

Figure 14. Prediction formula: (**a**) Absorption process and (**b**) desorption process.

6. Mathematical Modeling

Since the sample of the desiccant solution is contained in a small cylindrical beaker, the only important axis is the depth. However, the distribution of the solution concentration concerning radial and azimuthal axes is uniform, assuming isothermal walls. Moreover, the model represents all the expected physics in these phenomena. It contains a phase-change term, coupled with the empirical equation, in addition to the energy equation, which is necessary for the desorption case.

The $CaCl_2$ moisture absorption depends on water vapor sorption at the phase boundary between the air and the solution and $CaCl_2$ diffusion in the water. However, it is a slow process compared to the water vapor diffusion in the air. By neglecting the diffusion of $CaCl_2$ in water and considering the case of a thin layer solution, solving the calculations will be easier. A one-dimensional mathematical model in the z-direction is therefore proposed. A system of two transport (mass conservation) equations can solve the sorption phenomena; however, to solve the desorption process, a heat equation is needed:

$$\frac{\partial \rho_v}{\partial t} = D_v \frac{\partial^2 \rho_v}{\partial x^2} - \dot{m}, \tag{7}$$

$$\rho_s \frac{\partial \theta}{\partial t} = \dot{m} \tag{8}$$

$$c\rho_s \frac{\partial T_{sol}}{\partial t} = K \frac{\partial T_{sol}}{\partial x} \tag{9}$$

where ρ_v is the water vapor density [kg/m^3], D_v is the water vapour diffusion coefficient in the solution [m^2/s], ρ_s is the density of water-$CaCl_2$ mixture [kg/m^3] and c and K are the solution-specific heat and thermal conductivity, respectively. The transfer term $\dot{m}$ represents the mass transfer between vapor and liquid equation equations. We suggest the following definition of $\dot{m}$,

$$\dot{m} = -b(\theta_t - \theta_{max}) \tag{10}$$

In order to close the system of equations, it has been linked to the proposed empirical equations,

$$\theta_{max} = (c_1\ P_w + c_2)(1 + \frac{\ln \tau}{\ln \tau + c_3}) \tag{11}$$

$$\tau = \frac{T_{amb}}{T_{sol} - 273.15} \tag{12}$$

$$P_w = \frac{\rho_v R T_{sol}}{M} \tag{13}$$

where θ_{max}, b, τ, T_{amb}, T_{sol}, P_w are defined in the previous section (Section 5), c_1, c_2 and c_3 are defined in Table 2, R is the ideal gas constant 8.3136 [J $\cdot$ K^{-1} $\cdot$ mol^{-1}] and M is the molar mass of water 0.018 [kg/mol].

The initial conditions for Equations (7)–(9) are considered uniform and expressed in Equations (14)–(16), but the boundary conditions are defined only for the water vapor and solution temperature for Equations (7) and (9) in the Equations (17)–(20).

Initial conditions:

$$\rho_v\ (x, t = 0) = \rho_v^0 \tag{14}$$

$$\theta\ (x, t = 0) = \theta^0 \tag{15}$$

$$T_{sol}\ (x, t = 0) = T_{sol}^0 \tag{16}$$

Boundary conditions:

Upper Boundary

$$\rho_v\ (x = 0, t) = \rho_v^{air} \tag{17}$$

$$T_{sol}\ (x = 0, t) = T_{heat\_pad} \tag{18}$$

Lower Boundary

$$\frac{\partial \rho_v}{\partial x}(x = L, t) = 0 \tag{19}$$

$$\frac{\partial T_{sol}}{\partial x}(x = L, t) = 0 \tag{20}$$

where ρ_v^0 is the water vapor density related to the relative humidity at the surface of the solution and θ^0 is the mass ratio of water-to-$CaCl_2$ related to the initial concentration of the solution. T_{sol}^0 is the solution temperature and usually equals ambient temperature, T_{heat_pad} is the temperature of the controllable heat pad (set to high temperatures to mimic solar heating for desorption), ρ_v^{air} is the water vapor density related to the ambient relative humidity of the surrounding airflow [kg/m^3] and d is the depth of the solution [m].

The above highly nonlinear parabolic partial differential equation is solved numerically using an efficient algorithm. The governing Equations (7)–(13) are solved along with their initial and boundary conditions (14–20). The Galerkin method handles spatial discretization,

while an adaptive time step is used with time integration. The model is solved by using the "pdepe" function in MATLAB software that can solve a system of parabolic and elliptic partial differential equations. The pdepe is capable of solving the differential-algebraic equations that arise when the PDE contains elliptic equations by using the ode15 s solver, and for handling Jacobians with a specified sparsity pattern. Figure 15 shows the modeling results for both absorption/desorption processes.

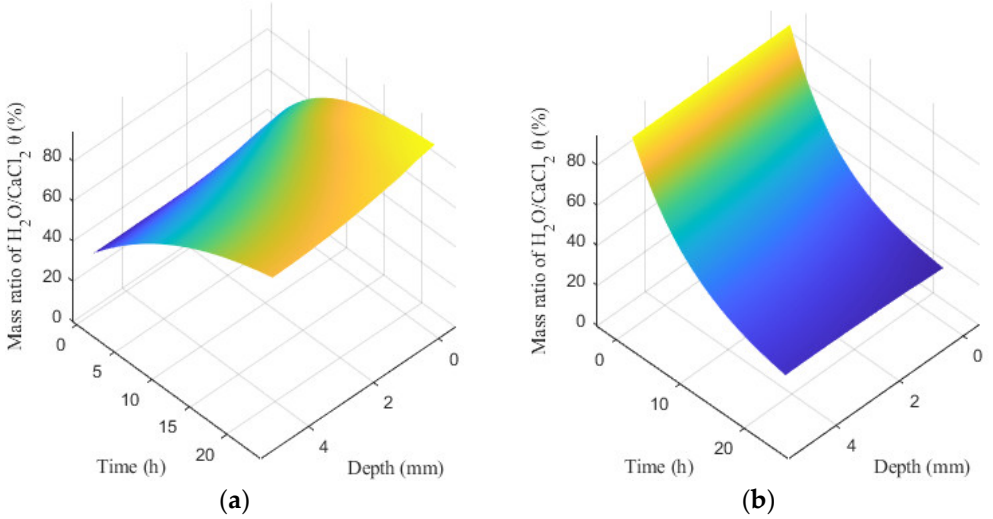

Figure 15. Mathematical model: (**a**) Absorption at 25 °C and (**b**) desorption at 50 °C.

The actual readings from the thin layer $CaCl_2$ solution are compared with the mathematical model in Figure 16. In the absorption process, the initial conditions for θ, ρ_v and T were set to 17%, 0.011 kg/m^3 (around 48% relative humidity), and 26.6 °C, respectively. The boundary condition for ρ_v only is set as 0.011 kg/m^3, since we assumed the temperature of the solution remains constant, and the MAE was determined to be 3.13%. In the desorption process, the initial conditions for θ, ρ_v and T were set to 89%, 0.011 kg/m^3, and 25.6 °C, respectively. The boundary conditions for ρ_v and T were set as 0.011 kg/m^3 and 45 °C, respectively. Since the solution is at a high temperature, and the model only considers the average temperature and relative humidity of the air around the solution, regardless of the forced convection applied to air at the surface of the solution, this results in a less accurate θ_{max} equation than the absorption model, so the model's MAE was calculated to be 7.32%.

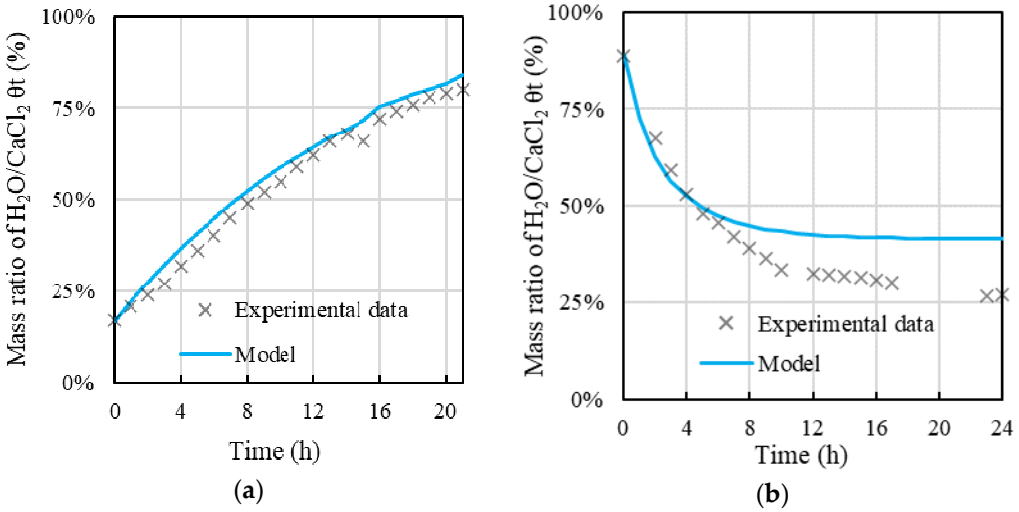

Figure 16. Actual against model (**a**) absorption at 25 °C and (**b**) desorption at 45 °C.

7. Simulation Scenarios

Various simulation scenarios of water absorption and desorption were performed using the proposed mathematical model to approximate the amount of water that could potentially be generated in the city of Jeddah, KSA. Table 3 shows the average values for day/night temperatures, relative humidity, and nighttime hours in Jeddah, used as data inputs for the model. The solution temperature is assumed to match the temperature during the daytime and the condensation temperature is the same as the ambient temperature at night.

Table 3. Simulation scenarios (data source: [38]).

Average Values	Summer (July)	Fall (October)	Winter (January)	Spring (April)
Day temperature (°C)	39	37	29	35
Night temperature (°C)	27	24	19	22
Relative humidity (%)	52	66	60	56
Nighttime (Hours)	9	10	11	10

The initial amount of water in the solution changed in each simulation until we ended with the same amount, to complete the absorption/desorption cycle. Figure 17 shows the simulation results of one day (one cycle) in each season. Assuming all desorbed water is condensed to water, the maximum amount that can be collected is in Fall, which equates to the highest relative humidity average in Table 3, and around 37% of the $CaCl_2$ mass. This means that an amount of 370 mL of water can be collected from 1 kg of $CaCl_2/m^2$ day at a depth of between 1.6–2.0 mm.

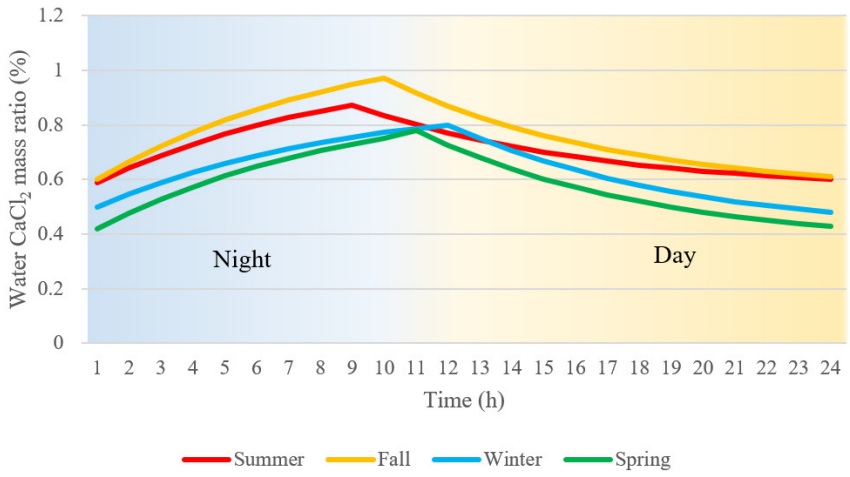

Figure 17. Seasonal simulation scenarios in Jeddah, KSA.

Changing the amount of desiccant will need more depth per m^2 and it will reduce the absorbed water ratio, as shown in Figure 18. Since the initial mass ratio is fixed, each increase in the depth means doubling the amount of $CaCl_2$ in the solution, yet the absorbed amount is less than double.

The simulation shows a linear relationship between collected water and depth of the solution (see Figure 19). A total of 1800 g of $CaCl_2$ can absorb 2160 mL of water from an area of 3 m^2 at 1 mm depth, but the same 1800 g of $CaCl_2$ can absorb only 630 mL if the area is 1 m^2 at 3 mm depth. This shows the importance of finding a solution to increase the absorption and desorption in deep containers. Adopting a thin layer approach for designing future AWG devices will consume vast areas and may complicate the maintenance process.

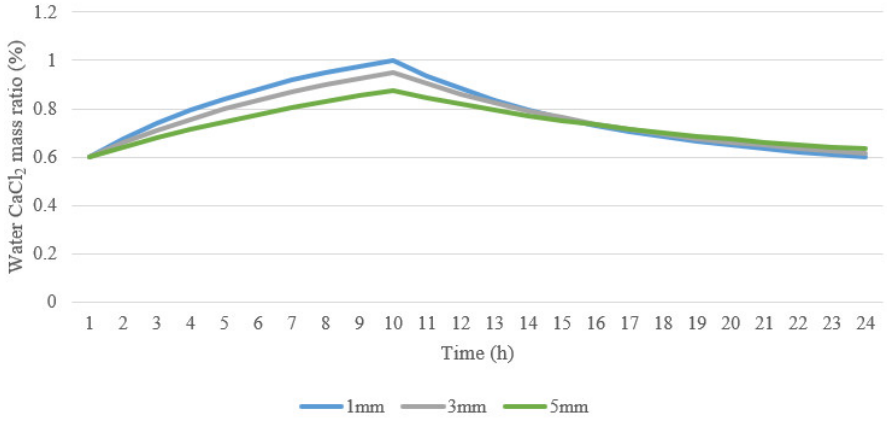

Figure 18. The effect of solution depth on absorption/desorption in fall.

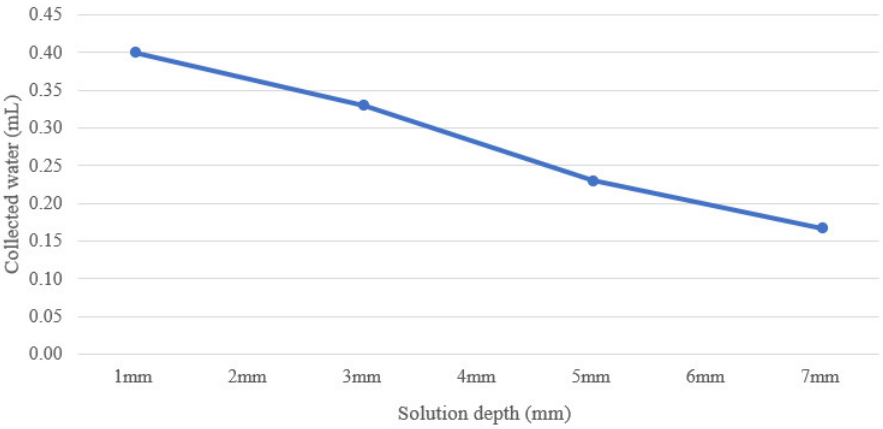

Figure 19. The effect of solution depth on collected water.

8. Conclusions

The conventional renewable source of freshwater is under high stress due to the growing global population. Atmospheric water and seawater desalination are promising renewable water sources, yet only a few countries can afford desalination due to the high cost and high energy consumption. Conventional AWGs that operate by active cooling to dew point consume even more energy. The promising solar regenerated desiccant-based AWG provides energy-efficient freshwater. This study conducted experiments on the desiccant, Calcium Chloride, to find ways to improve its absorption/desorption ability, where the uncertainty did not exceed ±3.5%. It was found that when using an air pump, it increased the absorption in deep containers; however, the use of a thin layer is still more effective. The results demonstrated high amounts of desorbed water in an open system. An empirical formula was proposed to describe the behavior of a heated thin layer of $CaCl_2$. The formula's MAE was calculated to be 1.9% and 3.56% for absorption and desorption, respectively. The model is dependent on the saturation point in an open system, θ_{max}, concluding that the model can predict the mass–moisture ratio efficiently. Furthermore, a one-dimensional mathematical model coupling three differential equations (mass and energy conservation) was derived and compared with experimental data; the MAE of the model was found to be 3.13% and 7.32% for absorption and desorption, respectively.

Author Contributions: Conceptualization, M.F.E.-A.; Data curation, I.K.A.; Formal analysis, M.F.E.-A.; Investigation, A.A. and I.K.A.; Methodology, A.A. and M.F.E.-A.; Resources, T.B.; Validation, A.A. and M.F.E.-A.; Writing—original draft, A.A.; Writing—review & editing, I.K.A., M.F.E.-A. and T.B. All authors have read and agreed to the published version of the manuscript.

Funding: The authors gratefully acknowledge the support of DGSR at Effat University, Jeddah, Saudi Arabia, for the Internal Grant No. UC#9/1June2022/7.1-21(4)3, Code: S2022-14-3.

Institutional Review Board Statement: Not Applicable.

Informed Consent Statement: Not Applicable.

Data Availability Statement: Not Applicable.

Conflicts of Interest: The authors declare no conflict of interest.

References

1. Mekonnen, M.M.; Hoekstra, A.Y. Four Billion People Facing Severe Water Scarcity. *Sci. Adv.* **2016**, *2*, e1500323. [CrossRef]
2. Global Change Ecology; da Silva, E.S.; Case, A. *The SDGs Series (Goal 6): Clean Water and Sanitation for All*; University of Bayreuth: Bayreuth, Germany, 2022.
3. World Bank Group. *High and Dry: Climate Change, Water, and the Economy*; World Bank: Washington, DC, USA, 2016.
4. Atmospheric Water Generator Market Size, Share, Report, 2027. Available online: https://www.fortunebusinessinsights.com/atmospheric-water-generator-market-103321 (accessed on 17 August 2022).
5. Ritchie, H.; Roser, M. *Water Use and Stress*; Our World in Data: Oxford, UK, 2017.
6. Introduction to the Water-Energy Nexus—Analysis. Available online: https://www.iea.org/articles/introduction-to-the-water-energy-nexus (accessed on 17 August 2022).
7. Lal, R. World Water Resources and Achieving Water Security. *Agron. J.* **2015**, *107*, 1526–1532. [CrossRef]
8. Jarimi, H.; Powell, R.; Riffat, S. Review of Sustainable Methods for Atmospheric Water Harvesting. *Int. J. Low-Carbon Technol.* **2020**, *15*, 253–276. [CrossRef]
9. Hanikel, N.; Prévot, M.S.; Yaghi, O.M. MOF Water Harvesters. *Nat. Nanotechnol.* **2020**, *15*, 348–355. [CrossRef]
10. Water Action Decade | Department of Economic and Social Affairs. Available online: https://sdgs.un.org/topics/water-and-sanitation/wateractiondecade (accessed on 17 August 2022).
11. Tu, Y.; Wang, R.; Zhang, Y.; Wang, J. Progress and Expectation of Atmospheric Water Harvesting. *Joule* **2018**, *2*, 1452–1475. [CrossRef]
12. Wang, Y.; Danook, S.H.; Al-bonsrulah, H.A.Z.; Veeman, D.; Wang, F. A Recent and Systematic Review on Water Extraction from the Atmosphere for Arid Zones. *Energies* **2022**, *15*, 421. [CrossRef]
13. Liu, X.; Beysens, D.; Bourouina, T. Water Harvesting from Air: Current Passive Approaches and Outlook. *ACS Mater. Lett.* **2022**, *4*, 1003–1024. [CrossRef]
14. Khalil, B.; Adamowski, J.; Shabbir, A.; Jang, C.; Rojas, M.; Reilly, K.; Ozga-Zielinski, B. A Review: Dew Water Collection from Radiative Passive Collectors to Recent Developments of Active Collectors. Sustain. *Water Resour. Manag.* **2016**, *2*, 71–86. [CrossRef]
15. Qadir, M.; Jiménez, G.C.; Farnum, R.L.; Dodson, L.L.; Smakhtin, V. Fog Water Collection: Challenges beyond Technology. *Water* **2018**, *10*, 372. [CrossRef]
16. Ge, T.S.; Xu, J.C. 13—Review of Solar-Powered Desiccant Cooling Systems. In *Advances in Solar Heating and Cooling*; Wang, R.Z., Ge, T.S., Eds.; Woodhead Publishing: Cambridge, UK, 2016; pp. 329–379. ISBN 9780081003015.
17. Bar, E. Extraction of Water from Air—An Alternative Solution for Water Supply. *Desalination* **2004**, *165*, 335. [CrossRef]
18. Bergmair, D.; Metz, S.J.; de Lange, H.C.; van Steenhoven, A.A. A Low Pressure Recirculated Sweep Stream for Energy Efficient Membrane Facilitated Humidity Harvesting. *Sep. Purif. Technol.* **2015**, *150*, 112–118. [CrossRef]
19. Zhuang, S.; Qi, H.; Wang, X.; Li, X.; Liu, K.; Liu, J.; Zhang, H. Advances in Solar-Driven Hygroscopic Water Harvesting. *Glob. Chall.* **2021**, *5*, 2000085. [CrossRef] [PubMed]
20. Talaat, M.A.; Awad, M.M.; Zeidan, E.B.; Hamed, A.M. Solar-Powered Portable Apparatus for Extracting Water from Air Using Desiccant Solution. *Renew. Energy* **2018**, *119*, 662–674. [CrossRef]
21. Sleiti, A.; Al-Khawaja, H.; Al-Khawaja, H.; Al-Ali, M. Harvesting Water from Air Using Adsorption Material -Prototype and Experimental Results. *Sep. Purif. Technol.* **2021**, *257*, 117921. [CrossRef]
22. Zhang, H.; Yuan, Y.; Sun, Q.; Cao, X.; Sun, L. Steady-State Equation of Water Vapor Sorption for CaCl2-Based Chemical Sorbents and Its Application. *Sci. Rep.* **2016**, *6*, 34115. [CrossRef]
23. Bhowmik, M.; Haldar, S.; Dharmalingam, K.; Muthukumar, P.; Anandalakshmi, R. Evaluation of Thermo-Kinetic and Absorption Characteristics of Pure Desiccants and Desiccant Mixtures. *Mater. Today Proc.* **2020**, *26*, 1967–1971. [CrossRef]
24. Elashmawy, M.; Alshammari, F. Atmospheric Water Harvesting from Low Humid Regions Using Tubular Solar Still Powered by a Parabolic Concentrator System. *J. Clean. Prod.* **2020**, *256*, 120329. [CrossRef]
25. Bouzenada, S.; Kaabi, A.N.; Frainkin, L.; Salmon, T.; Léonard, A. Experimental Comparative Study on Lithium Chloride and Calcium Chloride Desiccants. *Procedia Comput. Sci.* **2016**, *83*, 718–725. [CrossRef]
26. Elashmawy, M. Experimental Study on Water Extraction from Atmospheric Air Using Tubular Solar Still. *J. Clean. Prod.* **2020**, *249*, 119322. [CrossRef]
27. Kumar, M.; Yadav, A. Experimental Investigation of Solar Powered Water Production from Atmospheric Air by Using Composite Desiccant Material "CaCl2/Saw Wood". *Desalination* **2015**, *367*, 216–222. [CrossRef]

28. Srivastava, S.; Yadav, A. Water Generation from Atmospheric Air by Using Composite Desiccant Material through Fixed Focus Concentrating Solar Thermal Power. *Sol. Energy* **2018**, *169*, 302–315. [CrossRef]
29. Gandhidasan, P.; Abualhamayel, H. Investigation of Humidity Harvest as an Alternative Water Source in the Kingdom of Saudi Arabia. *Water Environ. J.* **2010**, *24*, 282–292. [CrossRef]
30. Conde, M.R. Properties of Aqueous Solutions of Lithium and Calcium Chlorides: Formulations for Use in Air Conditioning Equipment Design. *Int. J. Therm. Sci.* **2004**, *43*, 367–382. [CrossRef]
31. Garrett, D.E. *Handbook of Lithium and Natural Calcium Chloride*; Elsevier: Amsterdam, The Netherlands, 2004.
32. Milani, D.; Qadir, A.; Vassallo, A.; Chiesa, M.; Abbas, A. Experimentally Validated Model for Atmospheric Water Generation Using a Solar Assisted Desiccant Dehumidification System. *Energy Build.* **2014**, *77*, 236–246. [CrossRef]
33. Sibie, S.K.; El-Amin, M.F.; Sun, S. Modeling of Water Generation from Air Using Anhydrous Salts. *Energies* **2021**, *14*, 3822. [CrossRef]
34. Alkinani, S.; El-Amin, M.F.; Brahimi, T. Modeling and Numerical Analysis of Harvesting Atmospheric Water Using Copper Chloride. In Proceedings of the 6th International Conference on Green Energy and Applications, Singapore, 4–6 March 2022.
35. Temperature and Humidity Monitoring Expert. Available online: https://www.tzonedigital.com/en/about/3.aspx (accessed on 17 August 2022).
36. Huang, J. A Simple Accurate Formula for Calculating Saturation Vapor Pressure of Water and Ice. *J. Appl. Meteorol. Climatol.* **2018**, *57*, 1265–1272. [CrossRef]
37. Reduced Gradient—An Overview. ScienceDirect Topics. Available online: https://www.sciencedirect.com/topics/engineering/reduced-gradient (accessed on 17 August 2022).
38. Climate & Weather Averages in Jeddah, Saudi Arabia. Available online: https://www.timeanddate.com/weather/saudi-arabia/jeddah/climate (accessed on 17 August 2022).